Intrinsic Morphing of Compatible Triangulations

Vitaly Surazhsky Craig Gotsman

Center for Graphics and Geometric Computing
Department of Computer Science
Technion—Israel Institute of Technology

Abstract

Two planar triangulations with a correspondence between two vertex sets are compatible (*isomorphic*) if they are topologically equivalent. This work presents a simple and robust method for morphing two compatible planar triangulations with identical convex boundaries that locally preserves the intrinsic properties of triangles throughout the morph. The method is based on the barycentric coordinates representation of planar triangulations, and thus, guarantees compatibility of all intermediate triangulations. The intrinsic properties are preserved by interpolating angles and edge lengths components of *mean value* barycentric coordinates, rather than interpolating the barycentric coordinates. As a result, the method generates a natural-looking and guaranteed intersection-free morphing sequence.

Keywords: Controllable Morphing, Compatible triangulations, Morphing, Self-intersection elimination

1 Introduction

Morphing, also known as metamorphosis, is the gradual and continuous transformation of one shape (the *source*) into another (the *target*). Morphing has wide practical use in areas such as computer graphics, animation and modeling. To achieve more spectacular, impressive and accurate results, the morphing process requires a lot of the work to be done manually. A major research challenge is to develop techniques that will automate this process as much as possible.

The morphing problem has been investigated in many contexts, e.g., morphing of two-dimensional images [3, 12, 23], polygons and polylines [1, 4, 11, 12, 16–18], free-form curves [15] and even voxel-based volumetric representations [5]. The morphing process always consists of solving two main problems. The first one is to find a correspondence between elements (features) of the two shapes. The second problem is to find trajectories that corresponding elements traverse during the morphing process. Regrettably, a formal definition of a successful correspondence does not exist, as well as a definition of a successful solution of the trajectory problem. In this work we assume the more typical morphing scenario, namely, that the correspondence is given and only the trajectory problem is to be solved.

The naive approach to solve the trajectory problem is to choose the trajectories to be straight lines, where every feature of the shape travels with a constant velocity along its line towards the corresponding feature of the target during the morph. Unfortunately, this simple approach can lead to undesirable results. The intermediate shapes can vanish, i.e. degenerate into a single point, or contain self-intersections even though the source and target are simple, namely, self-intersection-free. Even if the linear morph is free of self-intersections and degeneracies, its intermediate shapes may have areas or distances between features far from those of the source and target, resulting in a "misbehaved" looking morph. Most of the research on solving the trajectory problem for morphing concentrates on trying to eliminate self-intersections and preserve the geometrical properties of the intermediate shapes. Many existing methods achieve good results for many inputs, however, none is able to guarantee any properties of the resulting morph.

Triangulations are ubiquitously used in computer graphics as a representation and a parameterization (e.g., for texture mapping) of surfaces and planar shapes. Two triangulations with a correspondence between their vertex sets are said to be compatible (*isomorphic*), if they are topologically equivalent. Floater and Gotsman [10] introduced an innovative approach for morphing compatible planar triangulations. This approach is based on the barycentric coordinates representation of planar triangulations. The morphing interpolation procedure is done in the space of barycentric coordinates, rather than in vertex geometry space. This approach is the only one, which applied to compatible triangulations with

identical boundaries, is able to analytically guarantee a continuous sequence of valid intermediate triangulations, namely, the triangulation does not self-intersect during the morph.

In [20], Surazhsky and Gotsman analyzed the basic approach for morphing compatible triangulations ([10]), investigated its properties and capabilities and presented several extensions that allow control over the properties of morphs. They showed that the basic approach has many degrees of freedom, which can be utilized in order to obtain morphs with various characteristics and still free from self-intersections. However, the schemes to obtain more natural morphs proposed in [20] are rather complicated and have problems inherent to the barycentric coordinates used in that work.

In this work we exploit the non-uniqueness of barycentric coordinates and use mean value barycentric coordinates that were recently introduced by Floater [9]. These coordinates preserve the shapes of triangles in a way similar to coordinates used in harmonic or conformal mappings [6]. However, the naive linear interpolation of mean value coordinates cannot guarantee that the shapes of triangles within intermediate triangulations transform uniformly, and thus, naturally. Mean value coordinates depends solely on triangle angles and edge lengths within a triangulation. In order to achieve a uniform transformation of the triangles shapes we interpolate angles and edge lengths of the corresponding triangles, and then use the intermediate values to get intermediate mean value coordinates.

Guaranteed intersection-free morphing of compatible planar triangulations allows morphing of any compatible piecewise linear objects such as polygons, polylines, tilings and so called stick figures as a general notion. Formally, *stick figures* are defined as connected straight-line plane graphs. Guaranteed intersection-free morphing of stick figures is achieved by embedding them as a subset of edges within compatible triangulations with identical boundaries. This embedding technique was introduced in [12] for polygons and extended in [21] for stick figures.

Constructing compatible triangulations for embedding of stick figures is a difficult problem and most of the existing algorithms [2, 13, 14, 21] produce triangulations that may have long, skinny and close to degenerate triangles together with many additional (*Steiner*) vertices. Moreover, the resulting compatible triangulations must usually be refined in order to create more natural morphing sequences, e.g. [1]. The refinement increases the number of vertices by a factor of 10–100 on the average, and this leads to very high computational cost of morphing sequences that can easily reach hours of CPU time even on modern 2-3GHz computers. In [22], a novel algorithm was introduced, which is able to construct compatible triangulations with a very small (close to optimal) number of Steiner vertices. However, having many of the triangles close to degenerate, the resulting compatible triangulation must be refined in order to be used with existing morphing algorithms.

The contribution of this paper is that our simple method produces natural morphing sequences between two planar compatible triangulations and is a robust method to obtain a natural morph between two stick figures. Our method is robust because the quality of the embedding triangulations used to morph two stick figures does not significantly affect the generated morphing sequence. Thus, our method can be applied to compatible triangulations with a very small number of Steiner vertices to obtain natural morphs in real time.

The paper is organized as follows: Section 2 introduces the notions of compatible triangulations and barycentric coordinates and define barycentric coordinates representation for triangulations. Section 3 shows how to produce a self-intersection free morph between compatible triangulations and then extends it to generate the intrinsic morph. Experimental results generated by our algorithm are shown in Section 4, and we conclude in Section 5.

2 Background

A simple graph $G = G(V, E)$ is a set of vertices $V = \{1, \ldots, |V|\}$ and a set of edges E, such that E is a subset of all unordered pairs of vertices $\{i, j\}$, when $i \neq j$. Two graphs G_0 and G_1 are *isomorphic* if there is a 1–1 correspondence between their vertices and edges in such a way that corresponding edges link corresponding vertices. A simple graph G is said to be *planar* if it can be drawn in the plane using simple curves for edges and the only intersections between the curves are at common endpoints standing for vertices. This representation of a planar graph G is called a *plane graph*, denoted by an ordered pair $(G, \wp)$. A mapping $\wp\colon V \to \mathbb{R}^2$ is a point sequence $\{i \mapsto (x_i, y_i) \mid i\colon 1, \ldots, |V|\}$. The following notations are equivalent and denote the coordinates of vertex i: $\wp(i)$, p_i, (x_i, y_i).

A plane graph partitions the plane into connected regions called *faces*. Obviously, a plane graph has a single unbounded face, denoted by the *outer* face. A plane graph is said to be *triangulated* if all its bounded faces have exactly three edges. A *planar triangulation* $\mathcal{T} = \mathcal{T}(G, \wp)$ is a simple triangulated plane graph such that its edges are represented by straight lines. We call a triangulation *valid* if it satisfies the above definition, in particular, the only intersections between its edges are at common endpoints.

Two (valid) triangulations are *isomorphic* if their planar graphs are isomorphic and the corresponding faces have the same orientation. To be consistent with other works, we also call isomorphic triangulations *compatible* triangulations. In this paper we will deal with compati-

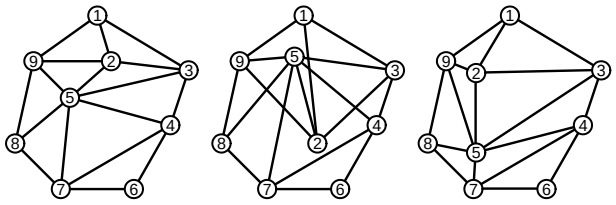

(**a**) (**b**) (**c**)

Figure 1: (**a**) Triangulation of 9 points in the plane. (**b**) Triangulation not compatible with (a). Vertex correspondence coded in digits. (**c**) Triangulation compatible with (a).

ble triangulations whose corresponding vertices have the same indices, namely, their planar graphs are identical. Thus, if $\mathcal{T}_0 = \mathcal{T}(G_0, \wp_0)$ and $\mathcal{T}_1 = \mathcal{T}(G_1, \wp_1)$ are compatible then $G_0 = G_1$. Figure 1 shows some compatible and non-compatible triangulations.

2.1 Barycentric Coordinates

Given a polygon with k vertices p_1, p_2, ..., p_k, $k \geq 3$, any point p in the plane can be expressed as:

$$p = \sum_{i=1}^{k} \lambda_i \cdot p_i, \quad \sum_{i=1}^{k} \lambda_i = 1. \tag{1}$$

The coefficients $\lambda_1, \ldots, \lambda_k$ in these equations are said to be *barycentric coordinates* of p relative to $p_1, \ldots, p_k$. When p lies in the convex hull of a polygon, it can be expressed as a convex combination of the polygon vertices, namely, all barycentric coordinates have positive values. In this paper we consider the case when p lies in the kernel of a star-shaped polygon.

In the special case when the polygon has three vertices, namely, p lies in a triangle $\triangle(p_1, p_2, p_3)$, the barycentric coordinates of p with respect to p_1, p_2, p_3 are uniquely determined by (1). Barycentric coordinates of p with respect to polygons with $k > 3$ vertices are not unique. A simple solution is to choose any triangle containing p whose vertices are vertices of the polygon. Barycentric coordinates of p now may be defined as non-zero coordinates with respect to the triangle vertices, and zeros for all other vertices. However, it has long been a challenging problem to find *strictly positive* barycentric coordinates that *continuously* and *smoothly* depend on p and the polygon vertices. Methods proposed by various works [6, 8, 19, 20] failed to satisfy at least one of the above requirements, and only recently Floater [9] solved this problem. He introduced the following simple formula for barycentric coordinates:

$$\lambda_i = \frac{w_i}{\sum_{j=1}^{k} w_k}, \quad w_i = \frac{\tan\left(\frac{\alpha_i}{2}\right) + \tan\left(\frac{\alpha_{i-1}}{2}\right)}{\ell_i}. \tag{2}$$

α_i is the angle at p of the triangle $\triangle(p, p_i, p_{i+1})$ and ℓ_i is the length of edge (p, p_i), namely, $\ell_i = \|p - p_i\|$.

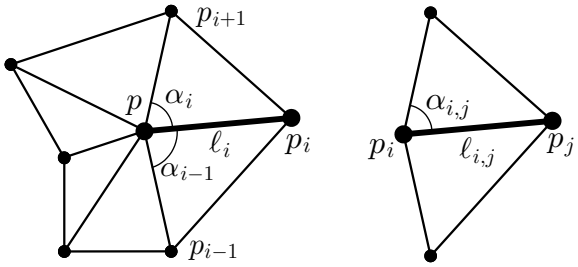

(a) (b)

Figure 2: Elements of mean value coordinates.

See Figure 2(**a**). Since $0 < \alpha_i < \pi$ being a triangle angle, it is easy to see that resulting barycentric coordinates are strictly positive. The barycentric coordinates defined in (2) are called *mean value* coordinates being inspired by the Mean Value theorem for harmonic functions. Mean value coordinates approximate harmonic maps by piecewise linear maps over triangulations.

2.2 Drawing Triangulated Graphs

It has been shown by Fáry [7] that every planar graph has a *straight line representation*. Hence, for every planar triangulated graph G, there exists a point sequence $\wp$ such that $\mathcal{T} = \mathcal{T}(G, \wp)$ is a (valid) triangulation. Tutte [24] described the following method to generate $\wp$: The boundary vertices of G are mapped to an arbitrary convex polygon with the same number of vertices and the same vertex order. Then, the interior vertices are placed such that every vertex is the centroid of its neighboring vertices. This scheme was extended by Floater [8]. Each interior vertex can be *any* convex combination of its neighbors. In terms of barycentric coordinates, any positive barycentric coordinates for each interior vertex may be chosen with respect to its neighbors.

To compute $\wp$, we use the following method. Let $G = G(V, E)$ be a simple triangulated graph, with $|V| = N$. We assume that boundary vertices of G have been identified. Let V_I be the set of the interior vertices and V_B be the set of the boundary vertices such that $|V_I| = n$ and $|V_B| = N - n = k$. Without loss of generality assume $V_I = \{1, \ldots, n\}$ and $V_B = \{n+1, \ldots, N\}$.

Now we wish to find coordinates of the graph vertices, namely, for each vertex $i \in V$ to find $\wp(i) = p_i = (x_i, y_i)$. We define $\wp$ for each vertex $i \in V_B$ to be coordinates of the vertices of a k-sided convex polygon.

For each interior vertex we may choose arbitrary non-negative barycentric coordinates relative to its neighbors, namely, for each vertex $i \in V_I$ a set of scalars $\lambda_{i,j}$ for $j = 1, \ldots, N$ such that

$$\begin{aligned} &\lambda_{i,j} = 0, \ \{i,j\} \notin E, \\ &\lambda_{i,j} \geq 0, \ \{i,j\} \in E, \end{aligned} \quad \begin{array}{c} \\ \text{barycentric coordinate} \\ \text{of } i \text{ relatively to } j. \end{array} \tag{3}$$

Next we define $p_1, \ldots, p_n$ to be the solution of the following system of linear equations

$$p_i = \sum_{i=1}^{N} \lambda_{i,j}\, p_j, \quad i = 1, \ldots, n. \tag{4}$$

This system contains n linear equations with n variables. It is shown in [8] that the corresponding matrix of these equations is non-singular. Therefore, a unique solution always exists. Thus, barycentric coordinates defined in (1) together with the locations of the triangulation boundary vertices uniquely determine the locations of the interior vertices. This representation is called *barycentric coordinates representation* of the triangulation.

3 Morphing Triangulations

A *morph* between two compatible triangulations $\mathcal{T}_0 = \mathcal{T}(G, \wp_0)$ and $\mathcal{T}_1 = \mathcal{T}(G, \wp_1)$ is a gradual transformation of $\mathcal{T}_0$ into $\mathcal{T}_1$. This transformation may be viewed as a continuous function $\mathcal{T}(t)$, $t \in [0,1]$ and $\mathcal{T}(0) = \mathcal{T}_0$, $\mathcal{T}(1) = \mathcal{T}_1$. A morph between $\mathcal{T}_0$ and $\mathcal{T}_1$ is *valid* if for all $t \in [0,1]$, $\mathcal{T}(t)$ is a valid triangulation compatible with $\mathcal{T}_0$. In this work we consider triangulations $\mathcal{T}_0$ and $\mathcal{T}_1$ such that the boundaries of the triangulations coincide. The boundaries of $\mathcal{T}(t)$ for $0 \le t \le 1$ will naturally also coincide. To find $\mathcal{T}(t)$ means to find $p_i(t)$ for $1 \le i \le n$ such that $\mathcal{T}(G, \wp_t)$ is compatible with $\mathcal{T}_0$.

Floater and Gotsman in [10] proposed to interpolate barycentric coordinates of the interior vertices of $\mathcal{T}_0$ and $\mathcal{T}_1$ rather than the interior vertex locations. Barycentric coordinates of $\mathcal{T}_0$ and $\mathcal{T}_1$ can be any valid positive barycentric coordinates, but strictly positive mean value coordinates defined in (2) are currently the best choice due to their properties. Interpolating strictly positive barycentric coordinates yields strictly positive intermediate barycentric coordinates as well. The intermediate barycentric coordinates uniquely define valid intermediate triangulations, resulting in a valid morph. Formally, we denote barycentric coordinates defined in (3) for $\mathcal{T}_0$ and $\mathcal{T}_1$ as $\lambda_{i,j}(0)$ and $\lambda_{i,j}(1)$ respectively. Intermediate barycentric coordinates are denoted by $\lambda_{i,j}(t)$ for $0 < t < 1$ and defined as a simple linear interpolations:

$$\lambda_{i,j}(t) = (1-t) \cdot \lambda_{i,j}(0) + t \cdot \lambda_{i,j}(1). \tag{5}$$

3.1 Intrinsic Morphing

In this work we go one step further and linearly interpolate components of the mean value coordinates formula, namely, triangle angles and edge lengths, rather than just the mean value coordinates. Formally, instead of (5) we use:

$$\begin{aligned} \alpha_{i,j}(t) &= (1-t) \cdot \alpha_{i,j}(0) + t \cdot \alpha_{i,j}(1) \\ \ell_{i,j}(t) &= (1-t) \cdot \ell_{i,j}(0) + t \cdot \ell_{i,j}(1) \end{aligned} \tag{6}$$

and combine them into (2) to obtain $\lambda_{i,j}(t)$. $\ell_{i,j}$ is the length of edge (i,j) and $\alpha_{i,j}$ is the angle at vertex i adjacent from the left to edge $\{i,j\}$. See Figure 2(**b**). $\alpha_{i,j}(0)$, $\alpha_{i,j}(1)$ and $\ell_{i,j}(0)$, $\ell_{i,j}(1)$ are taken from $\mathcal{T}_0$ and $\mathcal{T}_1$ respectively.

The motivation behind this was an attempt to obtain as uniform as possible transformations of triangle angles and edge lengths throughout the morphing process. Since the mean value coordinates formula (2) is not linear in angles and edge lengths, the linear interpolation of mean value coordinates correspond to some strictly nonlinear transformations of the angles and edge lengths. This may results in transformations of triangle angles and edge lengths which are significantly far from uniform.

4 Experimental Results

In practice, morphing is performed more frequently on stick figures than on planar triangulations. Thus, the problem of morphing planar figures is reduced to that of morphing triangulations, and the edges that are not part of the figure are ignored in the resulting morph. Figures 3 and 4 shows morphs between two polylines, the shapes of the two letters U and S, and two stick figures, the shapes of a scorpion and a dragonfly. These examples have been embedded within compatible triangulations using techniques developed in [22]. Note that that the triangulations in Figure 3(**a**)–(**b**) and Figure 4(**a**)–(**b**) have many long and skinny triangles, since the number of Steiner vertices is close to minimal. On the other hand, the triangulations in Figure 3(**c**)–(**d**) do not contain long and skinny triangles, but have many Steiner vertices. The examples show that applying interpolation of barycentric coordinates on triangulations with long, skinny triangles generates strange-looking morphs, see Figure 3(**f**),(**g**) and Figure 4(**d**). Using the same technique on high quality triangulations produces rather natural morphs, see Figure 3(**h**),(**i**). However, while the given polylines can be viewed as an approximation of smooth curves, the intermediate polylines are no longer smooth, no matter what barycentric coordinates were used. On the other hand, the intrinsic morph produces natural morphs for high quality triangulations, see Figure 3(**k**) as well as for triangulations with long and skinny triangles, see Figure 3(**j**). Moreover, for both these morphs the polylines stay smooth throughout the morphing sequences.

5 Discussion and Conclusion

We have presented a simple, robust and efficient method for morphing compatible triangulations that can be used to produce very natural and guaranteed intersection-free morphing sequences between stick figures. The quality

and behavior of the resulting morphs is not affected by the quality of the embedding triangulations. Even triangulations containing many triangles which are close to degenerate may be used to obtain natural morphs. This allows the use of compatible triangulations with a very small number of Steiner vertices, obtaining intersection-free natural morphs in almost real time.

It is important to emphasize the principal factor that makes it possible to obtain guaranteed intersection-free morphing of compatible triangulations and then to extend it to intrinsic morphing. The factor is changing representation of triangulations such that the interpolation space is extended. Namely, the main idea is to interpolate more elements in order to obtain better morphs. Using vertex locations gives $2n$ (x's and y's) degrees of freedom. Using barycentric coordinates involves $\sum_{i=1}^{n} d_i > 3n$ elements ($\approx 6n$ for large triangulations), where d_i is the degree of vertex i. The intrinsic morph interpolates $\sum_{i=1}^{n} d_i$ angles and $|E|-k$ edges, in total approximately $9n$ elements for large triangulations. Thus, every time the interpolation space is enlarged, morphs with more positive characteristics may be obtained.

REFERENCES

[1] Alexa, M., Cohen-Or, D., and Levin, D. As-rigid-as-possible polygon morphing. *Proceedings of SIGGRAPH '2000* (2000), 157–164.

[2] Aronov, B., Seidel, R., and Souvaine, D. L. On compatible triangulations of simple polygons. *Computational Geometry: Theory and Applications 3* (1993), 27–35.

[3] Beier, T., and Neely, S. Feature-based image metamorphosis. *Computer Graphics (SIGGRAPH '92) 26*, 2 (1992), 35–42.

[4] Carmel, E., and Cohen-Or, D. Warp-guided object-space morphing. *The Visual Computer 13* (1997), 465–478.

[5] Cohen-Or, D., Levin, D., and Solomovici, A. Three-dimensional distance field metamorphosis. *ACM Transactions on Graphics 17*, 2 (Apr. 1998), 116–141.

[6] Desbrun, M., Meyer, M., and Alliez, P. Intrinsic parameterizations of surface meshes. *Proceedings of EUROGRAPHICS 2002 21*, 2 (2002).

[7] Fáry, I. On straight line representation of planar graphs. *Acta Univ. Szeged Sect. Sci. Math. 11* (1948), 229–233.

[8] Floater, M. S. Parameterization and smooth approximation of surface triangulation. *Computer Aided Geometric Design 14* (1997), 231–250.

[9] Floater, M. S. Mean value coordinates. preprint.

[10] Floater, M. S., and Gotsman, C. How to morph tilings injectively. *Computational and Applied Mathematics 101* (1999), 117–129.

[11] Goldstein, E., and Gotsman, C. Polygon morphing using a multiresolution representation. *Proceeding of Graphics Interface* (1995), 246–254.

[12] Gotsman, C., and Surazhsky, V. Guaranteed intersection-free polygon morphing. *Computers and Graphics 25*, 1 (2001), 67–75.

[13] Gupta, H., and Wenger, R. Constructing piecewise linear homeomorphisms of simple polygons. *Journal of Algorithms 22*, 1 (1997), 142–157.

[14] Kranakis, E., and Urrutia, J. Isomorphic triangulations with small number of Steiner points. *International Jornal of Computational Geometry & Applications 9*, 2 (1999), 171–180.

[15] Samoilov, T., and Elber, G. Self-intersection elimination in metamorphosis of two-dimensional curves. *The Visual Computer 14* (1998), 415–428.

[16] Sederberg, T. W., Gao, P., Wang, G., and Mu, H. 2D shape blending: an intrinsic solution to the vertex path problem. *Computer Graphics (SIGGRAPH '93) 27* (1993), 15–18.

[17] Sederberg, T. W., and Greenwood, E. A physically based approach to 2D shape blending. *Computer Graphics (SIGGRAPH '92) 26* (1992), 25–34.

[18] Shapira, M., and Rappoport, A. Shape blending using the star-skeleton representation. *IEEE Trans. on Computer Graphics and Application 15*, 2 (1995), 44–51.

[19] Sugihara, K. Surface interpolation based on new local coordinates. *Computer-Aided Design 31* (1999), 51–58.

[20] Surazhsky, V., and Gotsman, C. Controllable morphing of compatible planar triangulations. *ACM Transactions on Graphics 20*, 4 (2001), 203–231.

[21] Surazhsky, V., and Gotsman, C. Morphing stick figures using optimized compatible triangulations. *Proceedings of Pacific Graphics* (Oct. 2001), 40–49.

[22] Surazhsky, V., and Gotsman, C. High quality compatible triangulations. *To appear in Proceedings of 11th International Meshing Roundtable* (2002).

[23] Tal, A., and Elber, G. Image morphing with feature preserving texture. *Computer Graphics Forum (Eurographics '99 Proceedings) 18*, 3 (1999), 339–348.

[24] Tutte, W. T. How to draw a graph. *Proc. London Math. Soc. 13* (1963), 743–768.

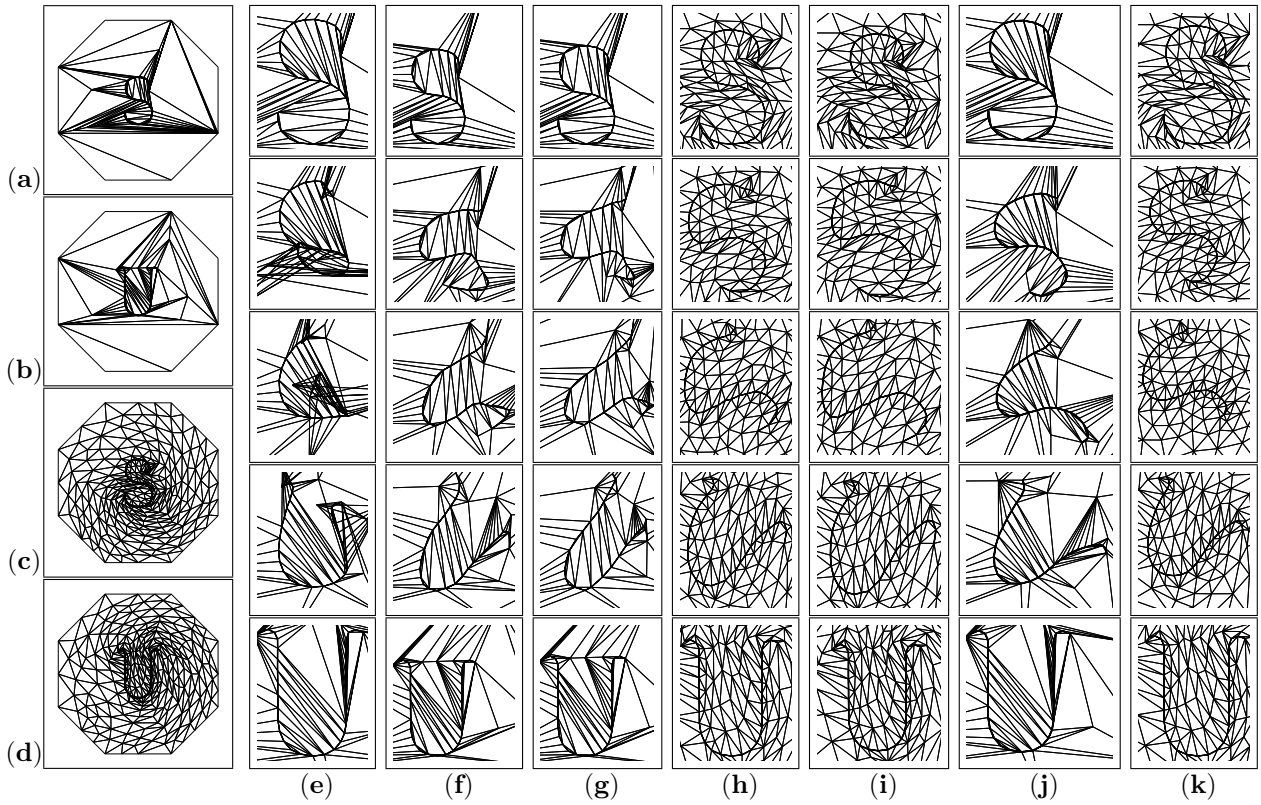

Figure 3: (**a**)–(**b**) Two polylines of letters U and S are embedded into compatible triangulations with 12 Steiner vertices. (**c**)–(**d**) The same polylines are embedded into high quality compatible triangulations with 186 Steiner vertices. (**e**) The linear interpolation of vertex positions results in an invalid morph. (**f**),(**g**) The linear interpolation of mean value (f) and minimal variance (g) [20] barycentric coordinates results in a valid but unnatural morph having a strange behavior of intermediate polylines. (**h**),(**i**) The linear interpolation of mean value (h) and minimal variance (i) [20] coordinates applied to high quality triangulations (c)–(d) produces a natural morph, however intermediate polylines is no longer smooth. (**j**) The intrinsic morph behaves naturally and has smooth intermediate polylines. (**k**) The intrinsic morph between high quality triangulations (c)–(d) is almost identical to (**h**).

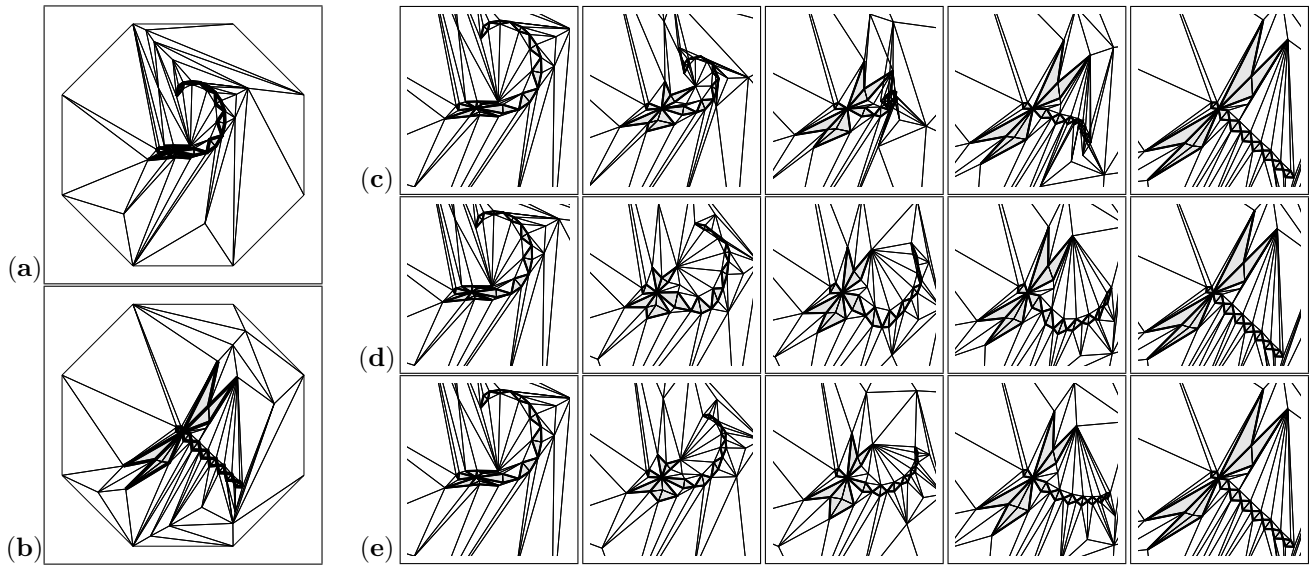

Figure 4: Morphing between figures of a scorpion and a dragonfly embedded into compatible triangulations: (**a**)–(**b**) Compatible embedding triangulations with only 11 Steiner vertices. (**c**) The linear interpolation of vertex positions results in an invalid morph. (**d**) The linear interpolation of mean value coordinates results in a valid but unnatural morph having a strange behavior of the tail part. (**e**) The intrinsic morph behaves naturally and has a smooth tail part in intermediate triangulations.